East European Journal of Physics. 4. 212–219 (2025)
DOI: 10.26565/2312-4334-2025-4-18 ISSN 2312-4334

SOLITARY WAVE AND SHOCK WAVE PERTURBATION FOR THE MODIFIED KAWAHARA EQUATION

Lakhveer Kaur[1], **Ahmed H. Arnous**[2,3], **Anjan Biswas**[4,5,6*]
[1]*Department of Mathematics, Jaypee Institute of Information Technology, Noida–201304, India*
[2]*Department of Mathematical Sciences, Saveetha School of Engineering, SIMATS, Chennai - 602105, Tamilnadu, India*
[3]*Research Center of Applied Mathematics, Khazar University, Baku, AZ 1096, Azerbaijan*
[4]*Department of Mathematics & Physics, Grambling State University, Grambling, LA 71245–2715, USA*
[5]*Department of Physics and Electronics, Khazar University, Baku, AZ–1096, Azerbaijan*
[6]*Department of Mathematics and Applied Mathematics, Sefako Makgatho Health Sciences University, Medunsa–0204, South Africa*
[*]*Corresponding Author e-mail: biswas.anjan@gmail.com*
Received September 1, 2025; revised October 14, 2025; accepted October 17, 2025

This paper retrieves shock waves and solitary wave solutions to the modified Kawahara equation in the presence of perturbation terms. The generalized G'/G–expansion approach is the adopted integration methodology for the model. The parameter constraints naturally emerge during the course of derivation of the solutions which guarantee the existence of such waves.

Keywords: *Integrability; G'/G–expansion; Parameter constraints*

PACS: 02.30.Jr; 05.45.Yv; 02.30.Ik; 47.40.Nm

1. INTRODUCTION

There are several popular models in shallow water waves that govern the dynamics of such flows along lake shores and sea beaches. A few such popular models are the Korteweg-de Vries (KdV) equation, the modifies KdV equation, Boussinesq equation, Camassa–Holmes equation [1–15]. Such equations have been studied in detail over the years and their solitary wave solutions as well as shock-like wave solutions have been retrieved. Their conservation laws have also been identified.

One additional model to address shallow water waves, is the Kawahara equation (KE) and the modified KE that predominantly models dispersive shallow water waves [1]. Lately, KE was addressed using the generalized G'/G–expansion approach, in presence of perturbation terms [6]. It must be noted that there exists several integration schemes that can recover solirary waves, shock waves and soliton solutions to a wide range of nonlinear evolution equations [16–20]. The current paper is a follow–up of the previous work on KE. The present work addresses the perturbed modified KE and the solitary waves and shock-like wave solutions are recovered with the implementation of the generalized G'/G–expansion scheme. The parameter constraints also emerged from this integration scheme during the course of the derivation of the solutions. Such parameter restrictions are an important necessity for the existence of the waves. The details are enumerated and exhibited in the rest of the paper.

The Kawahara and modified Kawahara equations are canonical dispersive models describing shallow-water, plasma, and optical pulse dynamics. Exact tanh- and coth-type solutions have been obtained for unperturbed or standard forms using analytic schemes such as generalized (G'/G), mapping, and bilinear-type methods [21–24]. In contrast, the present study investigates the *perturbed* modified Kawahara equation, where additional Hamiltonian-type and mixed-gradient terms modify the cubic nonlinearity and the fifth-order dispersion. Compared to earlier works, our analysis yields closed-form hyperbolic families constrained by explicit algebraic relations and reveals two distinct regimes $(m = 1)$ and $(m = 2)$ that differ in parameter freedom and tunability. We also examine how the discriminant $(\Theta = \lambda^2 - 4\mu)$ governs wave width and admissible parameter space (see Sections 2–4).

1.1. GOVERNING MODEL

An essential model for explaining the propagation of long waves in a variety of physical media, including shallow water, plasma, and nonlinear optical systems, is the modified KE, a dispersive nonlinear evolution equation that incorporates both cubic nonlinearity and higher-order dispersion. Richer wave phenomena, such as oscillatory solitons, non-monotonic wave profiles, and multi-soliton interactions, can be modeled with the modified form of the KE, which takes into account more intricate nonlinear interactions than the conventional version. Recent research has concentrated on achieving exact analytical solutions, such as solitary, periodic, and rational-type waves. Furthermore, the impact of nonlinearities and higher-order effects on the dynamics of wave propagation in realistic settings has been investigated using numerical simulations, modulation theory, and stability analysis.

Cite as: L. Kaur, A.H. Arnous, A. Biswas, East Eur. J. Phys. 4, 212 (2025), https://doi.org/10.26565/2312-4334-2025-4-18

KE is structured as:

$$q_t + a_1 q^2 q_x + a_2 q_{xxx} - a_3 q_{xxxxx} = 0, \tag{1}$$

here $a_1,\ a_2,\ a_3$ represents cubic nonlinear coefficient, third-order and fifth order dispersion coefficient respectively.

By adding physically relevant perturbation terms, we have introduced a perturbed form of the modified KE for the first time in this work. In practical physical contexts, when idealized assumptions are not true, these perturbations take into consideration the impacts of inhomogeneity, dissipation, and external influences. In addition to increasing the model's mathematical complexity, the addition of these components offers a more precise framework for examining the stability, evolution, and interaction of nonlinear dispersive waves in less than ideal circumstances.

The modified KE with perturbation terms is introduced as follows:

$$\begin{aligned} q_t + a_1 q^2 q_x + a_2 q_{xxx} - a_3 q_{xxxxx} = \theta q_x q_{xx} + \delta q^m q_x + \Lambda q q_{xxx} \\ + \nu q q_x q_{xx} + \xi q_x q_{xxx} + \psi q_{xxxxx} + \kappa q q_{xxxxx}, \end{aligned} \tag{2}$$

with $q = q(x,t)$, depicts amplitude of wave with independent variables t and x act as representing temporal and spatial variables.

2. MATHEMATICAL ANALYSIS

The perturbed modified KE (2) is investigated herein to find analytical solutions that demonstrate the impact of nonlinearity and higher-order dispersion in the presence of external factors. This analytical framework enables the construction of solitary, periodic, and rational-type solutions, providing deeper insight into how cubic nonlinearity, higher-order dispersion, and perturbative effects jointly influence the stability, amplitude, and velocity of nonlinear wave structures. We have implemented the generalized G'/G–expansion technique to model (2) in order to derive its exact solutions.

The considered model with perturbation terms (2) has been reduced to an ordinary differential equation in terms of the new variable $H(\sigma)$ by applying the wave transformation $\sigma = -\chi t + x$ and assuming a solution of the form with $q(x,t) = H(\sigma)$. This transformation simplifies the analysis of wave structures by basically converting the spatiotemporal dynamics into a stationary frame moving with wave speed χ. Consequently, the following ordinary differential equation is reduced from the modified KE (2):

$$\begin{aligned} &(-a_3 - \kappa H(\sigma) - \psi)\, H'''''(\sigma) + (a_2 - \xi H'(\sigma) - \Lambda H(\sigma))\, H'''(\sigma) + (-\nu H(\sigma) - \theta)\, H'(\sigma)\, H''(\sigma) \\ &+ \left(-\chi - \delta\, (H(\sigma))^m + a_1 H(\sigma)^2\right) H'(\sigma) = 0. \end{aligned} \tag{3}$$

A thorough strategic investigation of equation (2) has been done by utilizing the generalized G'/G–expansion technique. Then, after it yielded several solitary and shock-like wave solutions, equipped with free parameters. Given the complexity, nonlinearity, and computing demands of the model (2), this study is aimed at $m = 1,\ 2$, resulting into a variety of solutions with structured dynamics.

3. SOLITARY AND SHOCK-LIKE (SMOOTH KINK) WAVES

Throughout this section, the term "shock-like" refers to a shock-like smooth kink with a continuous tanh-type core. The steepness, proportional to $\sqrt{\Theta}$, is constraint-limited in Case I and tunable in Case II.

Case I ($m = 1$): condition ($\Theta > 0$)

Equation (2) has been recasted as follows after considering **m = 1** for find its explicit solutions:

$$\begin{aligned} &(-a_3 - \kappa H(\sigma) - \psi)\, H'''''(\sigma) + (a_2 - \xi H'(\sigma) - \Lambda H(\sigma))\, H'''(\sigma) + (-\nu H(\sigma) - \theta)\, H'(\sigma)\, H''(\sigma) \\ &+ \left(-\chi - \delta H(\sigma) + a_1 H(\sigma)^2\right) H'(\sigma) = 0. \end{aligned} \tag{4}$$

The following solution structure for equation (4) has been generated by appraising the homogeneous balance between its highest order derivative term and extremely nonlinear terms:

$$H(\sigma) = P_0 + P_1 \left(\frac{G'(\sigma)}{G(\sigma)}\right) + P_2 \left(\frac{G'(\sigma)}{G(\sigma)}\right)^2, \tag{5}$$

with $G(\sigma)$ satisfying following auxiliary equation:

$$G''(\sigma) + \lambda G'(\sigma) + \mu G(\sigma) = 0, \tag{6}$$

here, $P_i,\ i = 0, 1, 2$ are arbitrary parameters that need to be determined algebraically in mean computational process. The exact solutions of equation (2) are obtained by inserting the expression from (5) into equation (4), along with auxiliary condition (6) and followed by systematic collection of coefficients of similar powers of $\left(\frac{G'(\sigma)}{G(\sigma)}\right)$. The following parameter values are determined from the collection of algebraic relations, that this technique produced:

$$\begin{gathered}
\nu = -\tfrac{60\kappa}{P_2},\ \xi = -10\,\kappa\sqrt{\Theta},\ P_1 = \left(\lambda + \sqrt{\Theta}\right)P_2,\\
\theta = \tfrac{61\,\kappa\,P_2\lambda^2+24\,\kappa\,P_2\lambda\sqrt{\Theta}-168\,\psi-48\,\kappa\,P_0-196\,\mu\,\kappa\,P_2-3\,\Lambda\,P_2-168\,a_3}{2P_2},\\
a_1 = \tfrac{3(21\,\kappa\,P_2\lambda^2+24\,\kappa\,P_2\lambda\sqrt{\Theta}+\Lambda\,P_2-48\,a_3-48\,\psi-48\,\kappa\,P_0-36\,\mu\,\kappa\,P_2)}{{P_2}^2},\\
a_2 = -52\,\mu^2\kappa\,P_2 - 52\,\mu\,a_3 + \mu\,\Lambda\,P_2 - 52\,\mu\,\psi + 13\,a_3\lambda^2 + \Lambda\,P_0 + 13\,\psi\,\lambda^2 + 39\,\mu\,\kappa\,P_2\lambda^2 + 13\,\kappa\,P_0\lambda^2 - 52\,\mu\,\kappa\,P_0\\
-13/2\,\kappa\,P_2\lambda^4 - 13/2\,\kappa\,P_2\lambda^3\sqrt{\Theta} + 26\,\mu\,\kappa\,P_2\lambda\sqrt{\Theta} - 1/2\,\Lambda\,P_2\lambda^2 - 1/2\,\Lambda\,P_2\lambda\sqrt{\Theta},\\
\delta = -\tfrac{Z_1}{{P_2}^2},\ \chi = -\tfrac{Z_2}{2{P_2}^2},\ \Theta = \lambda^2 - 4\,\mu,
\end{gathered}\tag{7}$$

with

$$\begin{aligned}
Z_1 = {} & 2\mu\Lambda P_2^2 + \Lambda P_2^2\lambda^2 + 24\psi P_2\lambda^2 - 6\Lambda P_0P_2 + 24a_3P_2\lambda^2 - 384\mu\psi P_2\\
& - 296\mu^2\kappa P_2^2 - 384\mu a_3P_2 + 61\kappa P_2^2\lambda^4 - 98\mu\kappa P_2^2\lambda^2 - 102\kappa P_0P_2\lambda^2\\
& - 168\mu\kappa P_0P_2 + 84\mu\kappa P_2^2\lambda\sqrt{\Theta} - 288\kappa P_0\lambda P_2\sqrt{\Theta}\\
& + 51\kappa P_2^2\lambda^3\sqrt{\Theta} - 144\psi\lambda P_2\sqrt{\Theta} - 144a_3\lambda P_2\sqrt{\Theta}\\
& + 3\Lambda\lambda P_2^2\sqrt{\Theta} + 288P_0a_3 + 288P_0\psi + 288P_0^2\kappa,
\end{aligned}\tag{8}$$

and

$$\begin{aligned}
Z_2 = {} & -13P_2^3\lambda^5\kappa\sqrt{\Theta} - 24\psi\lambda^3P_2^2\sqrt{\Theta} - 24a_3\lambda^3P_2^2\sqrt{\Theta}\\
& - \Lambda\lambda^3P_2^3\sqrt{\Theta} + 552\mu\kappa P_0\lambda P_2^2\sqrt{\Theta} - \Lambda\lambda^4P_2^3\\
& - 13P_2^3\lambda^6\kappa + 288P_0^2a_3 + 288P_0^2\psi + 288P_0^3\kappa + 48\psi P_2^2\lambda^4 + 10\Lambda P_2^3\mu^2\\
& - 6\Lambda P_0^2P_2 + 96\mu^2a_3P_2^2 + 344\mu^3P_2^3\kappa + 96\mu^2\psi P_2^2 + 48a_3P_2^2\lambda^4\\
& - 340\mu\kappa P_0P_2^2\lambda^2 + 6\Lambda\lambda P_2^2P_0\sqrt{\Theta} - 2\Lambda\lambda P_2^3\mu\sqrt{\Theta}\\
& - 432\kappa P_0^2\lambda P_2\sqrt{\Theta} - 288P_0\psi\lambda P_2\sqrt{\Theta} - 288P_0a_3\lambda P_2\sqrt{\Theta}\\
& + 384\mu a_3\lambda P_2^2\sqrt{\Theta} - 118\mu\kappa P_2^3\lambda^3\sqrt{\Theta} + 248\mu^2\kappa P_2^3\lambda\sqrt{\Theta}\\
& + 78\kappa P_0\lambda^3P_2^2\sqrt{\Theta} + 384\mu\psi\lambda P_2^2\sqrt{\Theta} - 144\mu\psi P_2^2\lambda^2\\
& - 144\mu a_3P_2^2\lambda^2 + 48P_0P_2\lambda^2a_3 + 48P_0P_2\lambda^2\psi - 768P_0\mu a_3P_2\\
& - 768P_0\mu\psi P_2 + 170\kappa P_0P_2^2\lambda^4 - 496\mu^2\kappa P_0P_2^2 + 418\kappa\mu^2P_2^3\lambda^2\\
& - 92\mu\kappa P_2^3\lambda^4 - 78\kappa P_0^2P_2\lambda^2 - 552\kappa P_0^2P_2\mu + 2\Lambda P_0P_2^2\lambda^2\\
& + 4\mu\Lambda P_0P_2^2,
\end{aligned}\tag{9}$$

equipped with $\psi,\ \Lambda,\ P_0,\ P_2,\ \kappa$ as all free parameters in acquired parameter values.

By replicating (5) using the solution of equation (6) and parameter values found in (7), and then transforming to original variables $x,\ t$, the following solution structure for equation (2) has been retrieved.

The solution structure for equation (2) has been determined as follows:

$$\begin{aligned}
q\,(x,\ t) = {} & \left(\lambda + \sqrt{\Theta}\right)P_2\left(\frac{\sqrt{\Theta}\left(w_1\sinh\left(\frac{1}{2}\,\sigma\sqrt{\Theta}\right) + w_2\cosh\left(\frac{1}{2}\,\sigma\sqrt{\Theta}\right)\right)}{2\,w_2\sinh\left(\frac{1}{2}\,\sigma\sqrt{\Theta}\right) + 2\,w_1\cosh\left(\frac{1}{2}\,\sigma\sqrt{\Theta}\right)} - \frac{1}{2}\,\lambda\right)\\
& + P_0 + P_2\left(\frac{\sqrt{\Theta}\left(w_1\sinh\left(\frac{1}{2}\,\sigma\sqrt{\Theta}\right) + w_2\cosh\left(\frac{1}{2}\,\sigma\sqrt{\Theta}\right)\right)}{2\,w_2\sinh\left(\frac{1}{2}\,\sigma\sqrt{\Theta}\right) + 2\,w_1\cosh\left(\frac{1}{2}\,\sigma\sqrt{\lambda^2 - 4\,\mu}\right)} - \frac{1}{2}\,\lambda\right)^2,
\end{aligned}\tag{10}$$

here $w_1,\ w_2$ as arbitrary parameters and $\sigma = x - \chi t$ with χ given by (7).

Category–I: We have set up parameters choices as w_1 to zero and $w_2 \neq 0$ in order to find singular solitary wave solutions from the obtained solution (10) for equation (2). The resultant solution offers important information on the behavior of solution structures under particular physical conditions, featuring soliton dynamics.

$$q(x,t) = P_0 + \left(\lambda + \sqrt{\Theta}\right) P_2 \left(\frac{1}{2}\sqrt{\Theta}\coth\left(\frac{1}{2}(x-\chi t)\sqrt{\Theta}\right) - \frac{1}{2}\lambda\right) + P_2 \left(\frac{1}{2}\sqrt{\Theta}\coth\left(\frac{1}{2}(x-\chi t)\sqrt{\Theta}\right) - \frac{1}{2}\lambda\right)^2. \tag{11}$$

Category–II: By taking a particular values into consideration for the parameters $w_1 \neq 0$ and $w_2 = 0$, the shock-like wave solutions are retrieved from the resultant solution (10). This results into a term elimination, making the expression simpler and increases the dominance of nonlinear steepening, as a crucial aspect of shock-like wave production.

$$q(x,t) = P_0 + \left(\lambda + \sqrt{\Theta}\right) P_2 \left(\frac{1}{2}\sqrt{\Theta}\tanh\left(\frac{1}{2}(x-\chi t)\sqrt{\Theta}\right) - \frac{1}{2}\lambda\right) + P_2 \left(\frac{1}{2}\sqrt{\Theta}\tanh\left(\frac{1}{2}(x-\chi t)\sqrt{\Theta}\right) - \frac{1}{2}\lambda\right)^2. \tag{12}$$

All hyperbolic-type families considered here require $\Theta > 0$. The algebraic consistency relations summarized in (7) tie λ and μ (hence Θ) to the remaining coefficients; therefore Θ is *not freely tunable* but acts as a constraint on admissible parameter sets. Consequently, the inverse width $\sqrt{\Theta}$—and thus the steepness of the coth/tanh cores in (10)–(12)—is fixed once a feasible coefficient set is chosen.

It is worth noting that the equation (3) results into more computationally demanding analysis and a significantly more complex equation structure due to the higher-order nonlinear term interacting with both third- and fifth-order dispersive effects, as well as the introduced perturbation terms. This enhances the degree of involved computations, leading to larger algebraic systems with multiple coupled nonlinear parameter relations that require higher end symbolic computations. Thus next in this study, equation (2) is analyzed with $m = 2$ for generating new exact solutions.

Case II ($m = 2$)**: condition** ($\Theta > 0$)

The equation (3) is recited as follows with $m = 2$:

$$(-a_3 - \kappa H(\sigma) - \psi) H'''''(\sigma) + (a_2 - \xi H'(\sigma) - \Lambda H(\sigma)) H'''(\sigma) + (-\nu H(\sigma) - \theta) H'(\sigma) H''(\sigma) + \left(-\chi - \delta\, (H(\sigma))^2 + a_1 H(\sigma)^2\right) H'(\sigma) = 0. \tag{13}$$

The homogeneous balancing method is being utilized for equation (13) in order to find a balance between the equation's highest-order linear derivative term and its highest-order nonlinear term. As a result, following solutions structure is being proposed for equation (13):

$$H(\sigma) = P_0 + P_1\left(\frac{G'(\sigma)}{G(\sigma)}\right) + P_2\left(\frac{G'(\sigma)}{G(\sigma)}\right)^2, \tag{14}$$

Here, $G(\sigma)$ is a function that satisfies the auxiliary equation (6), while $P_i,\ i = 0,1,2$ are arbitrary parameters that must be found via algebraic calculations. The expression (14) is substituted into equation (13) along with the auxiliary condition (6) and thenafter coefficients of like powers of $\left(\frac{G'(\sigma)}{G(\sigma)}\right)$ are collected, to produce the exact solutions of equation (2). As stated below, this process produces a set of algebraic relations from which the parameter values required for the solutions to exist are derived:

$$\begin{aligned}
&\chi = \tfrac{1}{252} P_2 \left(276\lambda^4\mu\kappa - 312\theta\lambda^2\mu - 23\lambda^6\kappa + 39\theta\lambda^4 + 624\theta\mu^2 - 1104\lambda^2\mu^2\kappa + 1472\mu^3\kappa\right), \\
&\nu = -\tfrac{60\kappa}{P_2},\ \ \psi = -\tfrac{32}{21}\kappa\mu P_2 + \tfrac{8}{21}\kappa\lambda^2 P_2 - \tfrac{1}{84}\theta P_2 - a_3, \\
&\xi = -10\kappa\sqrt{\Theta}, \Lambda = -\tfrac{1}{3}\kappa\left(4\mu - \lambda^2\right), \\
&\delta = \tfrac{-148\lambda^2\kappa + 592\kappa\mu - 12\theta + 7a_1 P_2}{7P_2}, \\
&P_0 = -\tfrac{7}{12}\lambda^2 P_2 + 4/3\, P_2\mu + \left(\tfrac{1}{2}\lambda + \tfrac{1}{2}\sqrt{\Theta}\right) P_2\lambda,\ \ P_1 = \left(\lambda + \sqrt{\Theta}\right) P_2, \\
&a_2 = -\tfrac{1}{252} P_2 \left(712\kappa\lambda^4 + 39\theta\lambda^2 + 11392\kappa\mu^2 - 156\theta\mu - 5696\kappa\lambda^2\mu\right),
\end{aligned} \tag{15}$$

accompanied by $P_2,\ a_3,\ a_1,\ \kappa,\ \theta$ as free parameters in obtained parameter values.

The relations reported in (15) allow additional freedom in choosing λ and μ, so $\Theta = \lambda^2 - 4\mu$ becomes a *design-tunable* quantity. Accordingly, $\sqrt{\Theta}$ directly controls the front steepness and packet width in the expressions (16)–(18): as $\Theta \downarrow 0^+$ the structures broaden, whereas larger Θ yields steeper, more localized profiles.

Rewriting (14) using the solution of equation (6) and parameter values (15), we have yielded the following solution structure for equation (2)

$$
\begin{aligned}
q\,(x,\ t) = \left(\lambda + \sqrt{\Theta}\right) P_2 &\left(\frac{\sqrt{\Theta}\left(w_1 \sinh\left(\frac{1}{2}\,\sigma\,\sqrt{\Theta}\right) + w_2 \cosh\left(\frac{1}{2}\,\sigma\,\sqrt{\Theta}\right)\right)}{2\,w_2 \sinh\left(\frac{1}{2}\,\sigma\,\sqrt{\Theta}\right) + 2\,w_1 \cosh\left(\frac{1}{2}\,\sigma\,\sqrt{\Theta}\right)} - \frac{1}{2}\,\lambda \right) \\
+ P_0 + P_2 &\left(\frac{\sqrt{\Theta}\left(w_1 \sinh\left(\frac{1}{2}\,\sigma\,\sqrt{\Theta}\right) + w_2 \cosh\left(\frac{1}{2}\,\sigma\,\sqrt{\Theta}\right)\right)}{2\,w_2 \sinh\left(\frac{1}{2}\,\sigma\,\sqrt{\Theta}\right) + 2\,w_1 \cosh\left(\frac{1}{2}\,\sigma\,\sqrt{\Theta}\right)} - \frac{1}{2}\,\lambda \right)^2,
\end{aligned}
\tag{16}
$$

here $w_1,\ w_2$ as arbitrary parameters and $\sigma = x - \chi t$ with χ given by (15).

Category–I: The singular solitary wave solutions are recovered from obtained solution (16) for equation (2), by taking into account $w_1 = 0$ and $w_2 \neq 0$ as follows:

$$
\begin{aligned}
q(x,t) = P_0 + \left(\lambda + \sqrt{\Theta}\right) P_2 \left(\frac{1}{2}\,\sqrt{\Theta} \coth\left(\frac{1}{2}\,(x - \chi t)\,\sqrt{\Theta}\right) - \frac{1}{2}\,\lambda\right) \\
+ P_2 \left(\frac{1}{2}\,\sqrt{\Theta} \coth\left(\frac{1}{2}\,(x - \chi t)\,\sqrt{\Theta}\right) - \frac{1}{2}\,\lambda\right)^2.
\end{aligned}
\tag{17}
$$

Category–II: Embedding the parameter values as $w_1 \neq 0$ and $w_2 = 0$ in solution (16), we have procured the shock-like wave solutions for equation (2) as described below:

$$
\begin{aligned}
q(x,t) = P_0 + \left(\lambda + \sqrt{\Theta}\right) P_2 \left(\frac{1}{2}\,\sqrt{\Theta} \tanh\left(\frac{1}{2}\,(x - \chi t)\,\sqrt{\Theta}\right) - \frac{1}{2}\,\lambda\right) \\
+ P_2 \left(\frac{1}{2}\,\sqrt{\Theta} \tanh\left(\frac{1}{2}\,(x - \chi t)\,\sqrt{\Theta}\right) - \frac{1}{2}\,\lambda\right)^2.
\end{aligned}
\tag{18}
$$

4. RESULTS AND DISCUSSION

In Case I ($m = 1$), perturbation-induced algebraic constraints fix (λ, μ, Θ), producing specialized localized or kink-type profiles with fixed inverse width ($\sqrt{\Theta}$). In Case II ($m = 2$), Θ remains tunable, enabling continuous adjustment of front steepness and packet width for a given background level (P_0). Physically, Case I corresponds to a calibrated medium with fixed material or flow properties, whereas Case II models a design scenario where front thickness and localization can be engineered.

Now, we interpret the closed–form families obtained in Secs. 3, quantify the parameter regimes under which each family exists, and relate the formulas to their physical content and to limiting or benchmark cases. Throughout we use the traveling coordinate $\sigma = x - \chi t$ with wave speed χ given by (7) for $m = 1$ and by (15) for $m = 2$, and the discriminant $\Theta = \lambda^2 - 4\mu$. The hyperbolic families discussed below require $\Theta > 0$.

For both $m = 1$ and $m = 2$ we obtained the ansatz

$$
H(\sigma) = P_0 + P_1\left(\tfrac{G'}{G}\right) + P_2\left(\tfrac{G'}{G}\right)^2, \qquad G'' + \lambda G' + \mu G = 0,
$$

with $P_1 = (\lambda + \sqrt{\Theta})P_2$ and $\Theta = \lambda^2 - 4\mu$. When $\Theta > 0$ the auxiliary solution yields the hyperbolic representation (10) (for $m = 1$) and (16) (for $m = 2$). Two canonical parameter selections

$$
(w_1, w_2) = (0,\ w_2 \neq 0), \qquad (w_1 \neq 0,\ 0)
$$

produce, respectively, the singular solitary profiles (11), (17) (with a coth core) and the *shock–type* or kink–like profiles (12), (18) (with a tanh core). A rigid shift $\sigma \mapsto \sigma - \sigma_0$ (absorbed into w_1, w_2) relocates the crest or front without altering amplitude or width.

The roles of the key parameters can be summarized as follows in prose. The coefficient P_2 scales the overall amplitude of the nonlinear part, while P_0 sets the background offset level. The parameter $\sqrt{\Theta}$ controls the inverse width of the wave; larger values of $\sqrt{\Theta}$ yield narrower structures. The sign and magnitude of κ couple the field q into the highest–order dispersion and appear explicitly in the algebraic constraints (7) and (15), thereby tuning both the steepening (shock) and localization (solitary) tendencies.

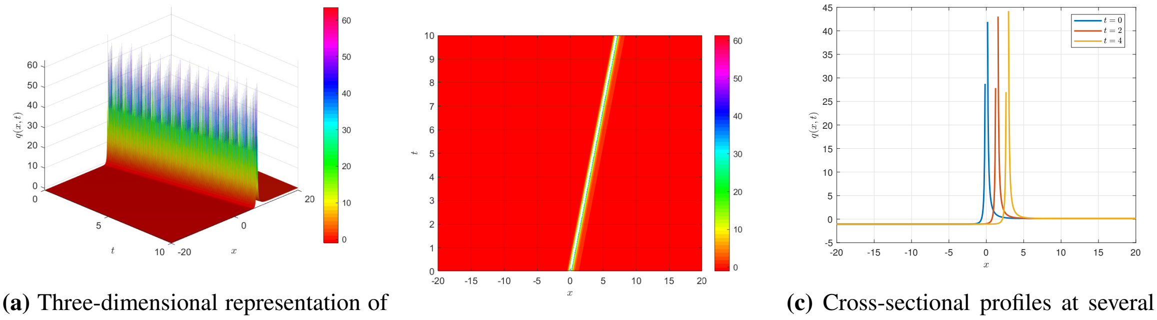

(a) Three-dimensional representation of $q(x,t)$.

(b) Contour illustration of $q(x,t)$.

(c) Cross-sectional profiles at several t values.

Figure 1. Category–I singular solitary wave pattern derived from Eq. (11).

Figure 1 illustrates the Category–I singular solitary wave solution of the perturbed modified Kawahara equation. Subfigure 1a shows the three-dimensional structure of $q(x,t)$, highlighting its strongly localized profile with sharp variations in amplitude. The contour plot in Subfigure 1b further emphasizes the persistence of this localized structure across the spatiotemporal domain. Cross-sectional in Subfigure 1c confirm that the wave maintains its shape over time, a defining property of solitary waves. Physically, these solutions represent stable energy packets arising from the balance between higher-order dispersion and cubic nonlinearity, relevant in shallow water dynamics, plasma propagation, and nonlinear optics.

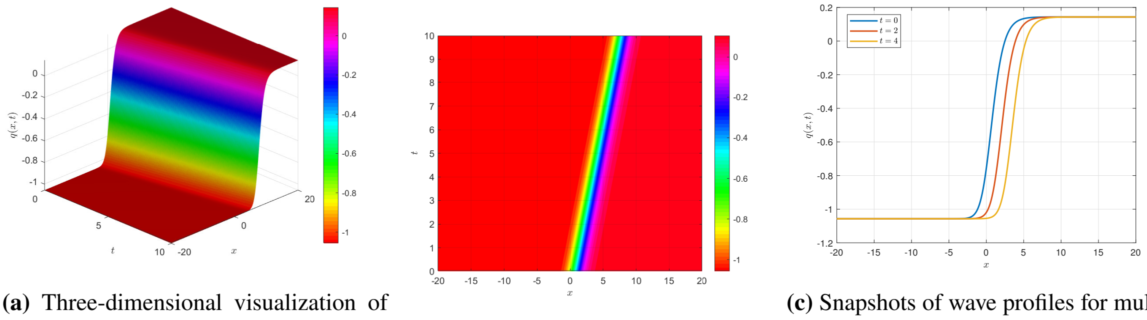

(a) Three-dimensional visualization of $q(x,t)$.

(b) Contour depiction of $q(x,t)$.

(c) Snapshots of wave profiles for multiple t values.

Figure 2. Category–II shock-type wave solution corresponding to Eq. (12).

Figure 2 presents the Category–II shock-type wave solution. The three-dimensional visualization in Subfigure 2a reveals the steep front of the shock profile, while the contour map in Subfigure 2b shows the abrupt transitions characteristic of nonlinear steepening. Subfigure 2c illustrate how these sharp wave fronts evolve over time. Physically, such solutions capture the role of strong nonlinearity and perturbative effects that drive shock formation, representing phenomena like breaking waves in hydrodynamics, compression waves in plasmas, and intense pulse propagation in nonlinear optical media. Together, Figures 1 and 2 demonstrate the contrasting interplay of dispersion and nonlinearity: the former yielding localized solitary waves, and the latter producing steep shock fronts under stronger nonlinear dominance. Figures 1 and 2 display the two canonical families for $m = 1$ (the $m = 2$ families have the same functional form with the speed and coefficients given by (15)).

The solution (11) (and (17)) is localized with an algebraic singularity at the center when $\sigma = 0$, reflecting a pole inherited from coth. Physically, this corresponds to a strongly localized structure supported by the balance of cubic nonlinearity and fifth–order dispersion, with the perturbations $(\theta, \delta, \Lambda, \nu, \xi, \psi, \kappa)$ renormalizing the amplitude, width, and speed. The singularity can be shifted off the physical domain by choosing the origin so that $\sigma \neq 0$ in the region of interest.

The solution (12) (and (18)) is a monotone front connecting two asymptotic states determined by $(P_0, P_2, \lambda, \Theta)$. Nonlinear steepening is reinforced by the mixed–gradient terms (θ, ν, ξ) and the q–dependent highest–order dispersion (κ), while fifth–order dispersion (a_3 and ψ) spreads the front, yielding a finite transition width proportional to $\Theta^{-1/2}$.

To clearly visualize the contrast between both studied regimes, a concise comparative summary is provided in Table titled "Summary Table: Case I vs. Case II". This table highlights the algebraic, structural, and physical differences between the two cases, emphasizing how tunability of Θ and wave localization properties distinguish the calibrated (Case I) and design–oriented (Case II) media.

Summary Table: Case I vs. Case II

Aspect	**Case I** ($m = 1$)	**Case II** ($m = 2$)
Consistency relations	Algebraic constraints summarized near Eq. (7)	Algebraic constraints summarized near Eq. (15)
Discriminant $\Theta = \lambda^2 - 4\mu$	Constrained by coefficients; $\Theta > 0$ restricts admissible sets	Effectively design-tunable (choose λ, μ so $\Theta > 0$)
Core profile	coth (singular solitary) Eq. (11); tanh (shock-like) Eq. (12)	coth Eq. (17); tanh Eq. (18)
Width / steepness	Fixed by $\sqrt{\Theta}$ (set by constraints)	Tunable via $\sqrt{\Theta}$ (design parameter)
Wave speed χ	Explicit relation from Eq. (7)	Explicit relation from Eq. (15)
Physical meaning	Calibrated medium with fixed material/flow properties (restricted set)	Design/tunable medium where front thickness and localization can be engineered

In the unperturbed limit, setting all perturbations to zero,

$$\theta = \delta = \Lambda = \nu = \xi = \psi = \kappa = 0,$$

reduces (2) to the modified Kawahara equation (1). In this limit the algebraic constraints collapse to the familiar relations for the pure modified KE and the hyperbolic families reduce to the standard tanh and coth profiles reported for the (modified) KE [1].

From (7) (for $m = 1$) and (15) (for $m = 2$), the wave speed χ is an explicit polynomial in (λ, μ) modulated by κ and by the perturbation strengths. Two robust qualitative trends hold. Increasing $\sqrt{\Theta}$, which produces narrower waves, increases $|\chi|$ when the k^5 dispersion $(a_3 + \psi)$ reinforces the cubic term (same sign), and decreases $|\chi|$ otherwise. This echoes the linear dispersion balance visible in $\omega(k)$. Moreover, positive κ, which strengthens the q–dependence in q_{xxxxx}, increases the magnitude of both steepening (Category–II) and localization (Category–I), manifesting in larger $|\xi|$ and $|\nu|$ via (7) and (15).

For reproducibility it is useful to summarize the most influential controls in narrative form. The wave width is set by $\sqrt{\Theta}$, and choosing λ, μ with $\lambda^2 - 4\mu$ large produces narrow structures. The amplitude scales with P_2, while P_0 shifts the baseline asymptote. The choice $(w_1, w_2) = (1, 0)$ yields shock–type tanh fronts, while $(0, 1)$ yields singular solitary coth pulses. The high–k tailing is controlled by $a_3 + \psi$, and changing its sign flips the curvature of $\omega(k)$ and the propensity for oscillatory overshoots near the front.

The perturbed terms in (2) also play clear roles. The terms $\theta q_x q_{xx}$ and $\nu q q_x q_{xx}$ enhance local steepening and promote shock formation (Category–II). The couplings $\Lambda q q_{xxx}$ and $\xi q_x q_{xxx}$ mediate nonlinear dispersive effects, modifying the front width and generating mild oscillations depending on the sign of $a_3 + \psi$. The ψq_{xxxxx} term renormalizes the fifth–order dispersion in the linear limit, directly influencing the selection of $\sqrt{\Theta}$ via the consistency relations. Finally, $\kappa q q_{xxxxx}$ couples amplitude to the highest–order dispersion and provides an additional lever to stabilize or destabilize steep structures without changing the background. These roles align with the contrasting morphologies shown in Figs. 1–2: dispersion versus nonlinearity determines whether energy remains localized (singular solitary waves) or organizes into a persistent transition layer (shock or kink).

5. CONCLUSIONS

The current paper recovered singular solitary wave and shock-like wave solutions to the perturbed modified KE. The perturbation terms are of Hamiltonian type which made this retrieval possible. The generalized G'/G–expansion scheme has made this retrieval possible along with the parameter constraints that guarantees the existence of such waves. It is visibly obvious of the shortcoming with this integration algorithm. The scheme fails to recover solitary wave solutions to the model. Therefore, later additional integration approaches will be adopted that would recover the solitary wave solutions in addition to the singular solitary waves and shock-like wave solutions. Such studies are under way and the results will be disseminated shortly.

Acknowledgments

This work of the last author (AB) was supported by Grambling State University for the Endowed Chair of Mathematics. The author thankfully acknowledges this support.

ORCID

Lakhveer Kaur, https://orcid.org/0000-0002-1936-474X; **Ahmed H. Arnous**, https://orcid.org/0000-0002-7699-7068; **Anjan Biswas**, https://orcid.org/0000-0002-8131-6044

REFERENCES

[1] A. Biswas, Appl. Math. Lett. **22**(2), 208–210 (2009). https://doi.org/10.1016/j.aml.2008.03.011

[2] A. Biswas, J. Vega-Guzman, A. Bansal, A.H. Kara, M. Aphane, Y. Yildirim, and H.M. Alshehri, Proc. Est. Acad. Sci. **72**(1), 17–29 (2023). https://doi.org/10.3176/proc.2023.1.03

[3] L. Kaur, Y. Yildirim, A.R. Adem, L. Moraru, and A. Biswas, Contemporary Mathematics (Wiser Publishers), **6**(2), 1756–1783 (2025). https://doi.org/10.37256/cm.6220256307

[4] L. Kaur, Y. Yildirim, A.H. Arnous, L. Moraru, A.M.K. Al-Dulaimi, A.S. Mahmood, and A. Biswas, Contemporary Mathematics (Wiser Publishers), **6**(3), 3715–3742 (2025). https://doi.org/10.37256/cm.6320256967

[5] L. Kaur, A. Biswas, A.H. Arnous, Y. Yildirim, L. Moraru, and M.J. Jweeg, Contemporary Mathematics (Wiser Publishers), **6**(3), 3743–3762 (2025). https://doi.org/10.37256/cm.6320256903

[6] L. Kaur, A.H. Arnous, I.Z. Chaloob, A.S. Mahmood, A.M.K. Al-Dulaimi, and A. Biswas, Submitted (Solitary waves and shock waves for the perturbed Kawahara equation).

[7] N.A. Kudryashov, and D.I. Sinelshchikov, Acta Appl. Math. **113**(1), 41–44 (2011). https://doi.org/10.1007/s10440-010-9582-6

[8] C.S. Liu, Comput. Phys. Commun. **181**(2), 317–324 (2010). https://doi.org/10.1016/j.cpc.2009.10.006

[9] A.D. Polyanin, and N.A. Kudryashov, Contemporary Mathematics (Wiser Publishers), **5**(4), 5783–5794 (2024). https://doi.org/10.37256/cm.5420245840

[10] X.Y. Tang, and S.Y. Lou, J. Math. Phys. **44**(9), 4000–4025 (2003). https://doi.org/10.1063/1.1598619

[11] A.M. Wazwaz, Chaos, Solitons Fractals, **196**, 116307 (2025). https://doi.org/10.1016/j.chaos.2025.116307

[12] A.M. Wazwaz, S.A. El-Tantawy, L.S. El-Sherif, A.S. Al-Johani, and H.A. Alyousef, Alexandria Eng. J. **123**, 1–16 (2025). https://doi.org/10.1016/j.aej.2025.03.035

[13] K. Manju, and A.M. Wazwaz, Chinese J. Phys. **93**, 515–530 (2025). https://www.sciencedirect.com/science/article/pii/S0577907324004878

[14] A.M. Wazwaz, Int. J. Numer. Model. Electron. Netw. Devices Fields, **38**(3), e70063 (2025). https://doi.org/10.1002/jnm.70063

[15] A.S. Rashed, T.A. Mahmoud, and A.M. Wazwaz, Waves Random Complex Media, **35**(2), 3662–3690 (2025). https://doi.org/10.1080/17455030.2022.2053611

[16] A.J.M. Jawad and M.J. Abu-AlShaeer, Al-Rafidain J. Eng. Sci. **1**(1), 1–8 (2023). https://doi.org/10.61268/sapgh524

[17] N. Jihad, and M.A.A. Almuhsan, Al-Rafidain J. Eng. Sci. **1**(1), 81–92 (2023). https://doi.org/10.61268/0dat0751

[18] A.J.M. Jawad, and A. Biswas, Al-Rafidain J. Eng. Sci. **2**(1), 43–50 (2024). https://doi.org/10.61268/2bz73q95

[19] I.M. Mendez-Zuniga, T.L. Belyaeva, M.A. Aguero, and V.N. Serkin, Transactions in Optics and Photonics, **1**(1), 22–33 (2025). https://ojs.wiserpub.com/index.php/top/article/view/5835

[20] Z. Kasapeteva, Transactions in Optics and Photonics, **1**(1), 58–66 (2025). https://ojs.wiserpub.com/index.php/top/article/view/6639

[21] A.M. Wazwaz, Phys. Lett. A, **360**(4–5), 588–592 (2007). https://doi.org/10.1016/j.physleta.2006.08.068

[22] T. Öziş and İ. Aslan, Appl. Math. Comput. **216**(8), 2360–2365 (2010). https://doi.org/10.1016/j.amc.2010.03.081

[23] A. Bekir, Phys. Lett. A, **372**(19), 3400–3406 (2008). https://doi.org/10.1016/j.physleta.2008.01.057

[24] K.A. Gepreel, J. Partial Differential Equations, **24**(1), 55–69 (2011). https://doi.org/10.4208/jpde.v24.n1.4

ЗБУРЕННЯ ОДИНОЧНОЇ ХВИЛІ ТА УДАРНОЇ ХВИЛІ ДЛЯ МОДИФІКОВАНОГО РІВНЯННЯ КАВАХАРИ

Лаквір Каур[1], Ахмед Х. Арнус[2,3], Анджан Бісвас[4,5,6]

[1] *Кафедра математики, Інститут інформаційних технологій Джайпі, Нойда–201304, Індія*
[2] *Кафедра математичних наук, Інженерна школа Савітха, SIMATS, Ченнаї - 602105, Тамілнад, Індія*
[3] *Науково-дослідний центр прикладної математики, Університет Хазар, Баку, Аризона 1096, Азербайджан*
[4] *Кафедра математики та фізики, Державний університет Гремблінга, Гремблінг, Луїзіана 71245–2715, США*
[5] *Кафедра фізики та електроніки, Університет Хазар, Баку, AZ–1096, Азербайджан*
[6] *Кафедра математики та прикладної математики, Університет медичних наук Сефако Макгатхо, Медунса–0204, Південна Африка*

У цій статті отримано розв'язки модифікованого рівняння Кавахари на основі ударних хвиль та одиночних хвиль за наявності членів збурень. Узагальнений підхід G'/G–розкладу є прийнятою методологією інтегрування для моделі. Обмеження параметрів природно виникають під час виведення розв'язків, які гарантують існування таких хвиль.

Ключові слова: *інтегрованість; G'/G–розклад; обмеження параметрів*